UNDERLYING TECHNOLOGY PROGRAMME 2004

PHYSICS INTEGRATION

TASK: UT-TPDC-IRRCER
Irradiation effects in ceramics for heating and current drive, and diagnostic systems

***Deliverables*: 1) The comparative study of gamma-ray, electron beam and neutron flux radiation effect on semiconductor lasers. 2) The evaluation of the optical absorption induced by gamma-ray and neutron radiation in solarization resistant optical fibres in the UV-visible range.**

D. Sporea, Adelina Sporea*, C. Oproiu*, B. Constantinescu** and I. Vata***

**National Institute for Laser, Plasma and Radiation Physics, Bucharest*
***"Horia Hulubei" National Institute of R&D for Physics and Nuclear Engineering, Bucharest*

Subtask objectives

Apart from optical fibre and free-space communications, laser diodes became primary radiation sources in interferometry, vibrometry, proximity sensors, spectroscopy, material processing and surface treatment, replacing more bulky and expensive gas and solid-state lasers. Some of their characteristics (small size, long operating life, easy to use and maintain, great diversity, low price) recommend them for remote sensing and robotic applications. All these operations are of interest for remote handling tasks and control in fusion installations (i.e. ITER, DEMO). Their use under irradiation conditions (gamma, neutron) is a real challenge, hence the interest on the study of these devices behaviour as they are subjected to irradiation. Further, there is a concern in relation to the radiation induced optical absorption in optical fibres as they have to be employed in fusion installations fiberscope.

Our research has been focalized on the following objectives:

- the comparative study of gamma-ray, electron beam and neutron flux radiation effect on semiconductor lasers;
- the evaluation of the optical absorption induced by gamma-ray and neutron radiation in solarization resistant optical fibres in the UV-visible range.

1. Gamma-ray, electron beam and neutron flux irradiation effect on semiconductor lasers

The report presents:

- the development of ***additional set-ups and the associated software*** to measure several new parameters for the laser diodes;
- the evaluation of ***gamma-ray, electron beam and neutron*** effects on two laser diodes emitting at 780 nm and 808 nm.
- the study of the degradation of the operating characteristics of two laser diodes ***emitting at communication wavelengths*** (1310 nm and 1550 nm).

1.1. The setup and the software programme used

The setup developed during previous years made possible the evaluation of almost all macroscopic parameters of laser diodes, function of the total irradiation dose and the laser driving conditions:

a) the optical power vs. the driving current of the semiconductor laser;
b) the wavelength of the emitted radiation vs. the driving current of the laser;
c) the embedded photodiode current vs. the emitted optical power;
d) the longitudinal mode structure of the emitted radiation vs. the driving current of the laser;
e) the transversal mode structure of the emitted beam vs. the driving current of the laser;
f) the temporal stability of the output optical power;
g) the temporal stability of the emitted radiation wavelength;
h) the peak and the centroid location of the optical power spatial distribution;
i) the laser point source stability;
j) the ellipticity of the emitted laser beam and the cross section of the beam profile.

The setup and the associated software programme implemented this year were used to assess:

a) the peak emission wavelength;
b) the centroid wavelength;
c) the spectral bandwidth of the emitted radiation;
d) the switch-on time of the output optical power;
e) the temporal stability of the spectrum of the emitted optical radiation.

1.2. Results concerning the irradiation of near-IR laser diodes

a. During the reporting period, the irradiation effects on two semiconductor lasers operating at λ = 780 nm and 808 nm were studied. The main results are illustrated below, for **gamma-ray, electron beam** and **neutron** irradiations. Only the extreme diode case temperature and total irradiation doses are considered for the simplicity of the representation. Data are available for ***all*** the irradiation steps. The irradiation conditions are given in the Table 1. All the irradiations were done at room temperature. The measurements were performed in the Laser Metrology and Standardization Laboratory, off-line, for various operating conditions (driving current and laser diode case temperature). [1], [2] The laser diode emitting at 780 nm was an index-guided

structure, while that operating at 898 nm was double heterostructure diode. Gamma-ray energy spectrum has two peaks at 1173 keV and at 1332 keV and dose rate: 0.33 kGy/h. Electron beam irradiation conditions were: dose rate: 200 krad/min; driving current: 2 μA; pulse duration: 3 μs; pulse frequency: 100 Hz; beam energy: 6 MeV. Neutron irradiation conditions were: neutron energy: 5.2 MeV (bell shape); production yield at 10 cm from the Be target: 2.13 x 10^8 n/cm^{2}s μA; deuteron beam intensity: 10 A; components of the mixed neutron/ gamma radiation: 138 Gy/C and 2.38 Gy/C.

Table 1. The irradiation steps for the laser diodes operating at near-IR wavelengths

Irradiation step	1	2	3	4	5	6	7	8	9
Total irradiation dose (MGy) for gamma-ray irradiation	0.27	0.34	0.44	0.6	0.76	0.96	1.16	1.28	1.36
Total irradiation dose (MGy) for electron beam irradiation	0.16	0.28	0.44	0.52	0.6	-	-	-	-
Maxim fluence (n/cm^2) for neutron irradiation	6 x 10^{11}	6 x 10^{12}	1.2 x 10^{13}	-	-	-	-	-	-

We have also studied the changes induced by neutron and gamma-ray irradiation on two quantum well semiconductor lasers operating at 1300 nm and 1550 nm, with no optical fiber attached to them.

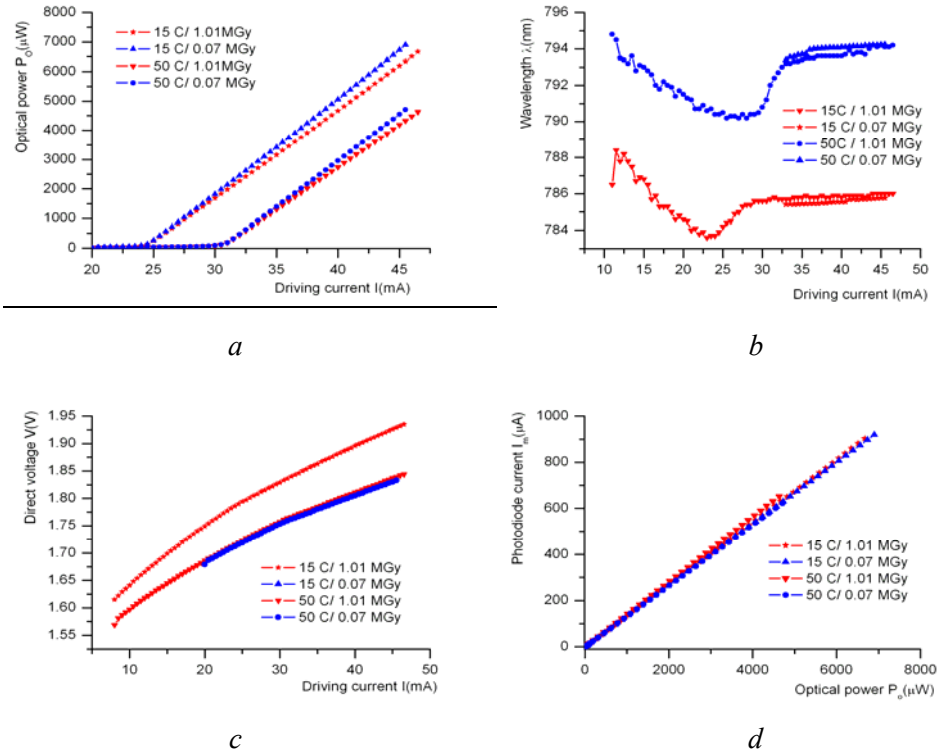

Figure 1. Irradiation effects on the index-guided laser diode emitting at 780 nm: a -the optical power vs. the driving current characteristics; b – the wavelength of the emitted radiation vs. the driving current characteristics; c – the direct voltage vs. the driving current characteristics; d – the photodiode current vs. the emitted optical power characteristics, for two gamma irradiation doses, at two case temperatures.

For the index-guided laser diode subjected to gamma irradiation (Figure 1) the irradiation induced a very small increase of the threshold current, as compared to the change produced by the increase of the case temperature that is of about 5 mA. The decrease of the external quantum efficiency is higher at lower case temperatures, after gamma irradiation. Above the threshold current, a slight increase of the emitted radiation wavelength occurs (0.2 nm). For this laser the degradation of the embedded photodiode reponsivity is very small, for the considered total irradiation doses.

In the case of neutron irradiation (Figure 2), the index-guided laser diode proves to be more affected, as its threshold current increases (up to 4 mA for the higher case temperature situation), the emitted radiation wavelength decreases by 7 nm below the threshold current value, and remains almost unchanged above the threshold current), while the embedded photodiode's responsivity decreases (i.e. the photocurrent at the fluence of 10^{13} n/cm^2 is 60 % of the value corresponding to a fluence of 10^{11} n/cm^2, at the same optical power of 6 mW).

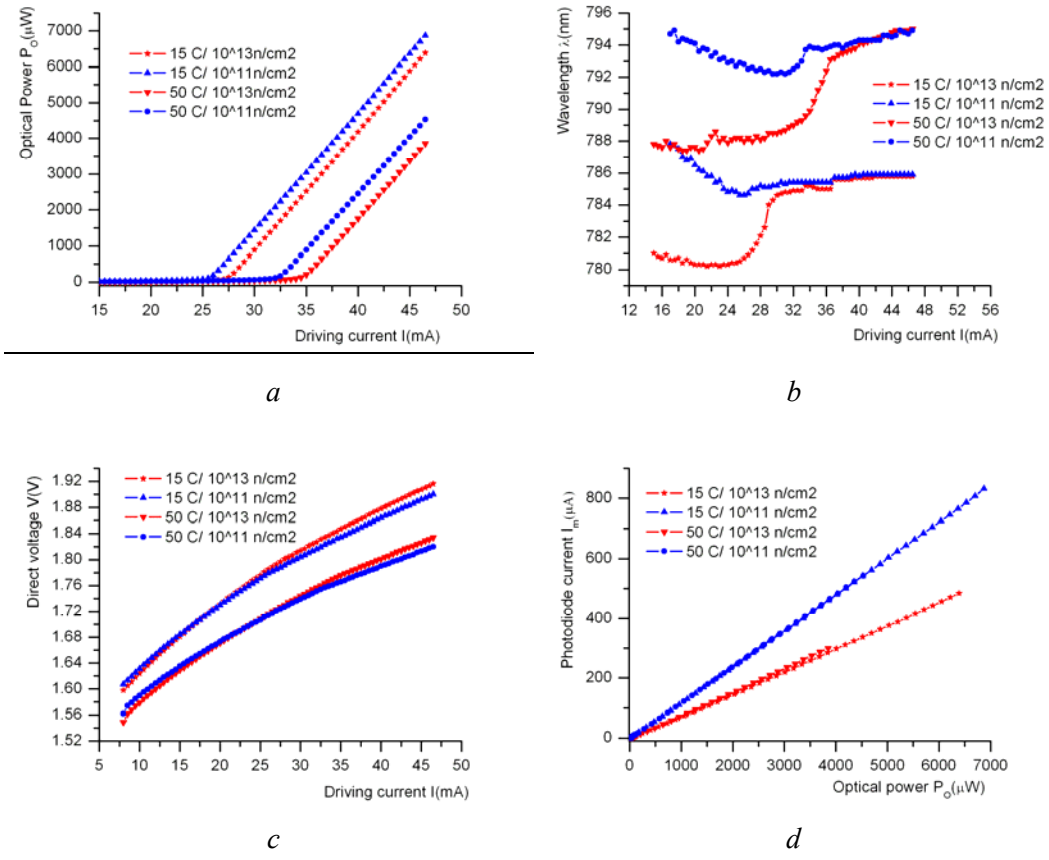

Figure 2. Irradiation effects on the index-guided laser diode emitting at 780 nm: a -the optical power vs. the driving current characteristics; b – the wavelength of the emitted radiation vs. the driving current characteristics; c – the direct voltage vs. the driving current characteristics; d – the photodiode current vs. the emitted optical power characteristics, for two neutron fluences, at two case temperatures.

The irradiation of this laser diode by an electron beam (Figure 3) increases (by 2 mA) the threshold current less than the neutron irradiation, has no effect over the emitted radiation wavelength, and produces a drop of about 30 % in the photodiode current at the emitted optical power of 5 mW.

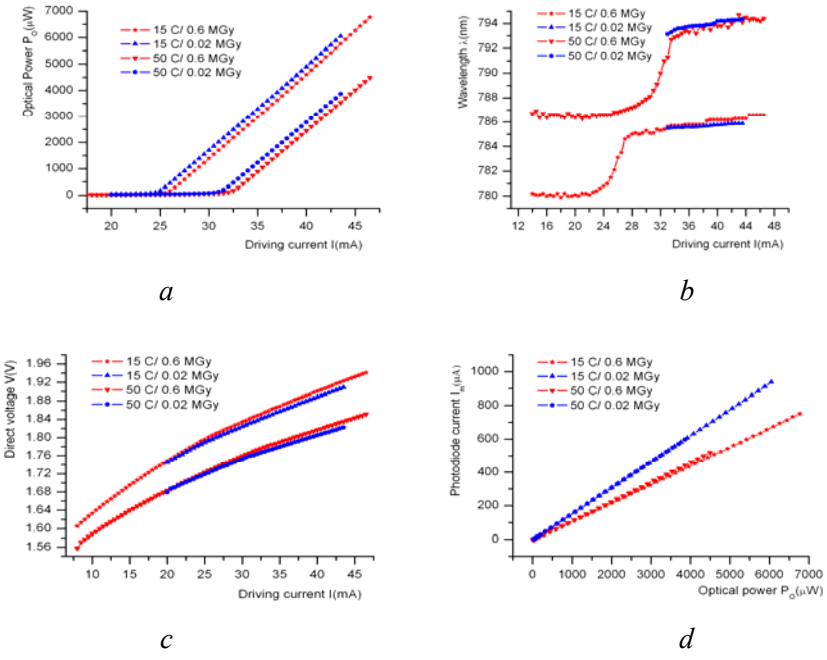

Figure 3. Irradiation effects on the index-guided laser diode emitting at 780 nm: a -the optical power vs. the driving current characteristics; b – the wavelength of the emitted radiation vs. the driving current characteristics; c – the direct voltage vs. the driving current characteristics; d – the photodiode current vs. the emitted optical power characteristics, for two total electron beam irradiation doses, at two case temperatures.

The following Figures illustrate the degradation of the laser diode emitting at 808 nm (double heterostructure) after gamma-ray, neutron and electron beam irradiation.

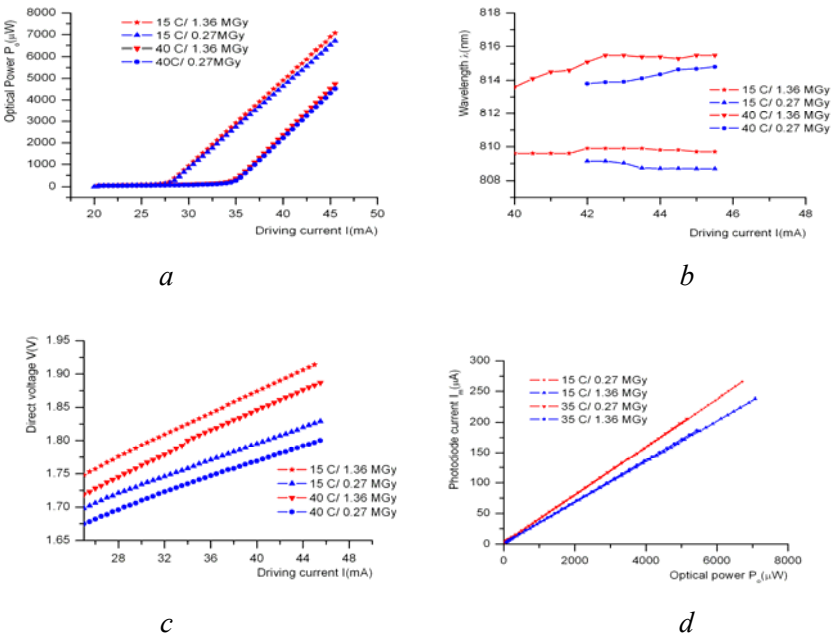

Figure 4. Irradiation effects on the double heterostructure laser diode emitting at 808 nm: a -the optical power vs. the driving current characteristics; b – the wavelength of the emitted radiation vs. the driving current characteristics; c – the direct voltage vs. the driving current characteristics; d – the photodiode current vs. the emitted optical power characteristics, for two gamma irradiation doses, at two case temperatures.

Gamma irradiation of this laser diode has little effect over its threshold current and external quantum efficiency (Figure 4). Above the threshold current, an increase of about 1 nm of the emitted radiation wavelength occurs, as well as an increase of the compliance voltage (i.e. 0.1 V at the driving current of 40 mA). For this semiconductor laser, gamma irradiation induces a decrease of the photodiode responsivity (i.e. a drop by 25 % for the case of 5 mW emitted optical power).

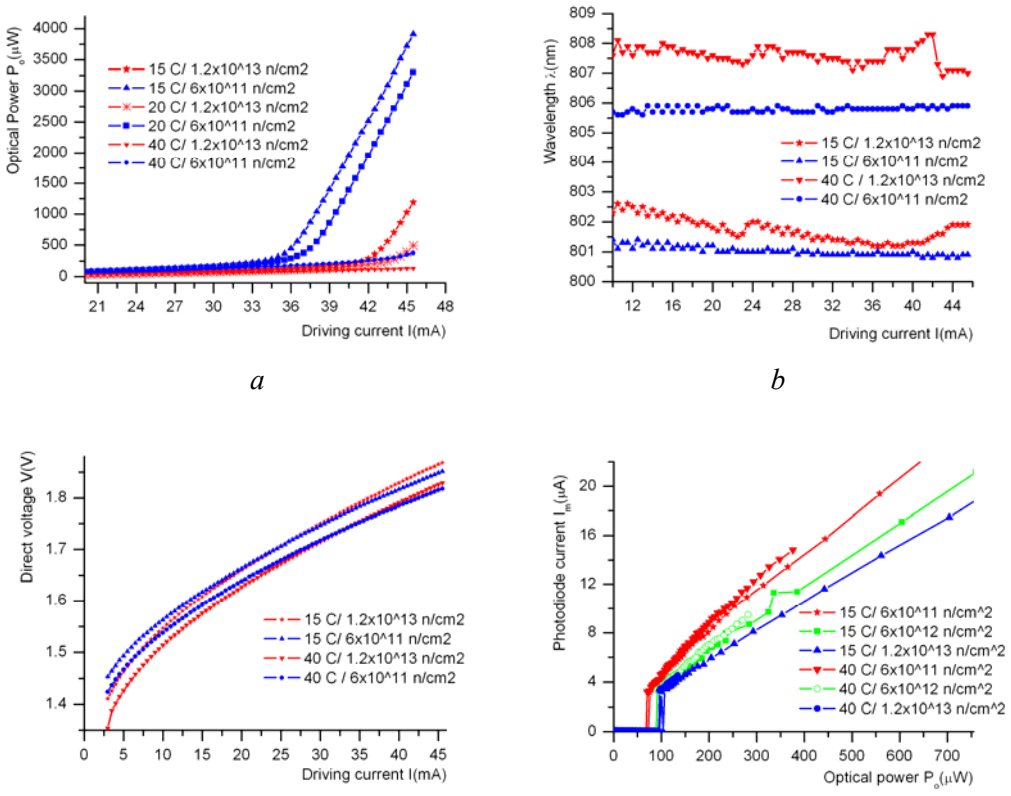

Figure 5 Irradiation effects on the double heterostructure laser diode emitting at 808 nm: a - the optical power vs. the driving current characteristics; b – the wavelength of the emitted radiation vs. the driving current characteristics; c – the direct voltage vs. the driving current characteristics; d – the photodiode current vs. the emitted optical power characteristics, for two neutron fluences, at two case temperatures.

Under neutron irradiation (Figure 5) this laser diode exhibits a noticeable increase of its threshold current (7 mA), and an increase of about 1 – 2 nm (depending on the case temperature) of the emitted radiation wavelength. At the case temperature of 15^{O}C the photodiode responsivity decreases with the increase of the neutron fluence, while at higher case temperatures its current is very small.

In the case of electron beam irradiation (Figure 6) the parameters most affected by the irradiation are the threshold current (5 mA). Small changes are registered as it concerns the emitted radiation wavelength and the photodiode responsivity.

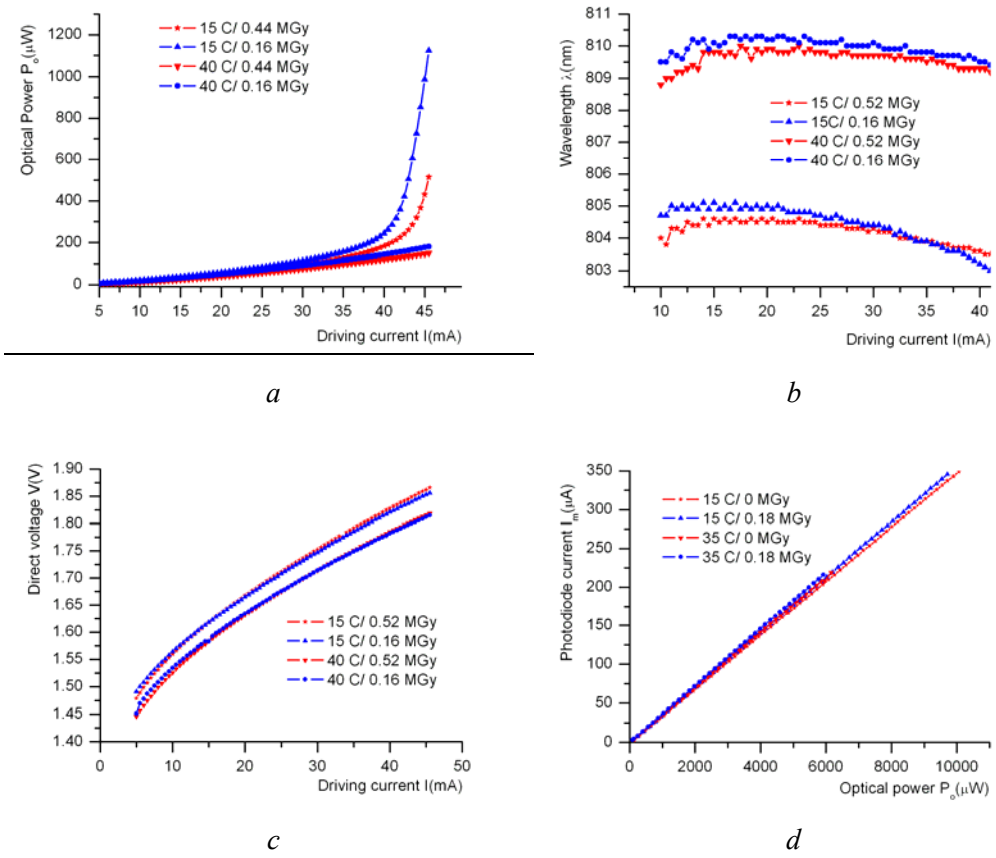

Figure 6. Irradiation effects on the double heterostructure laser diode emitting at 808 nm: a -the optical power vs. the driving current characteristics; b – the wavelength of the emitted radiation vs. the driving current characteristics; c – the direct voltage vs. the driving current characteristics; d – the photodiode current vs. the emitted optical power characteristics, for two total electron beam irradiation doses, at two case temperatures.

One laser diode was subjected to high driving current cycling after irradiation. The upper limit of the driving current was within the data sheets limits. The cycling was done for about one hour, at a case temperature of 15 ^{O}C. In these conditions, no significant changes were noticed in the output emitted optical power.

As compared to our previous work we performed this year some investigations concerning the emitted radiation spectral characteristics such as: peak wavelength and its temporal stability, centroid wavelength, full-half-bandwidth. These evaluations were done using a multi-channel optical fibre spectrometer, a laser diode driver and a temperature controller. A dedicated programme, developed in the Laboratory using the graphical programming environment LabVIEW, was used to remote control the laser diode operating parameters. The emitted laser radiation was captured with an integrating sphere, which in turn was coupled to the spectrometer through an optical fibre of 400 μm diameter. To evaluate the above mentioned laser parameters two software packages (OOIBase and OIIRad) were used, both purchased from the spectrometer producer.

As an example of the temporal variation of the longitudinal mode structure for the two investigated laser diodes, in Figures 7 and 8 is indicated the variation of the intensity for three wavelengths. From the recorded data the change in the peak emission wavelength and in the

laser diode's full-half-bandwidth can be deduced, as they are modified in time and with the laser driving conditions. In our case, the lasers were operated at the upper limit of their driving current, for the case temperature at its lower and upper limits. The recording time was about 15 min in each situation. For the spectrometer, the value for the box car parameter was 1, the integration time was 500 ms for the gamma irradiated diodes and 250 ms for the case of neutron irradiation. Figures 7 and 8 illustrate the results after neutron irradiation.

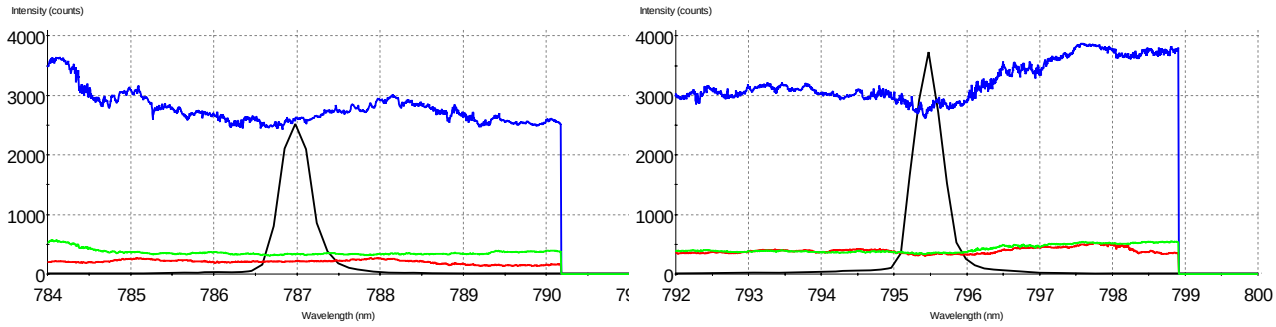

Figure 7. The change in the relative intensity of three wavelengths for the index-guide (780 nm), single mode laser diode, at a total neutron fluence of 2 x 10^{13} n/cm^2, a- for case temperature of T = 15 ^{O}C, the driving current of I = 46 mA. The monitored wavelengths were: λ_1(red) = 786.6 nm ; λ_2 (blue) = 787.0 nm; λ_3 (green) = 787.4 nm; b - for case temperature of T = 50 ^{O}C, the driving current of I = 46 mA. The monitored wavelengths were: λ_1(red) = 795.1 nm ; λ_2 (blue) = 795.5 nm; λ_3 (green) = 795.9 nm.

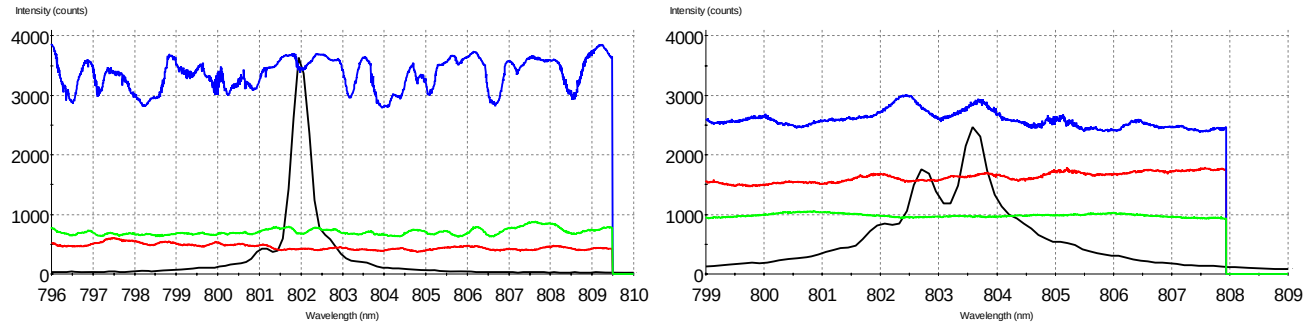

Figure 8. The change in the relative intensity of three wavelengths for the double heterostructure (808 nm), single mode laser diode, at a total neutron fluence of 2 x 10^{13} n/cm^2, a - for case temperature of T = 13 ^{O}C, the driving current of I = 47 mA. The monitored wavelengths were: λ_1(red) = 801,1 nm ; λ_2 (blue) = 801,9 nm; λ_3 (green) = 802,6 nm, the integration time was 450 ms; b - for case temperature of T = 20 ^{O}C, the driving current of I = 47 mA. The monitored wavelengths were: λ_1(red) = 802,75 nm ; λ_2 (blue) = 803,6 nm; λ_3 (green) = 804,4 nm; the integration time was 650 ms.

The double heterostructure laser presents a more instable operation as compared to the index-guided structure laser for both gamma-ray and neutron irradiation, as multimode structures builds up, both at low and at high case temperature.

1.3. Results concerning the irradiation of semiconductor lasers operating at communication wavelengths

The irradiation steps for two laser diodes, emitting at 1300 nm and 1550 nm, are given in Table 2. The irradiation was done at room temperature and the measurements were performed off-line.

Table 2. The irradiation steps for the laser diodes operating at communication wavelengths

Irradiation step	**1**	**2**	**3**
Total irradiation dose (MGy) for gamma-ray irradiation	0.02	0.1	0.18
Maximum fluence (n/cm^2) for neutron irradiation	10^{12}	10^{13}	-

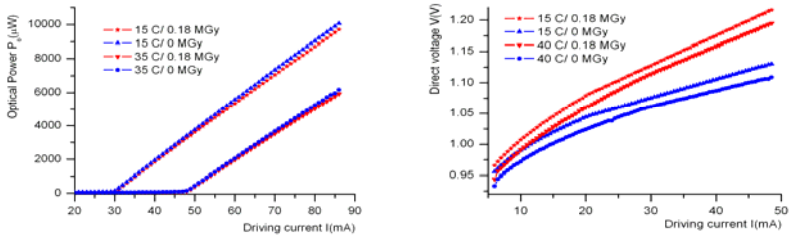

a *b*

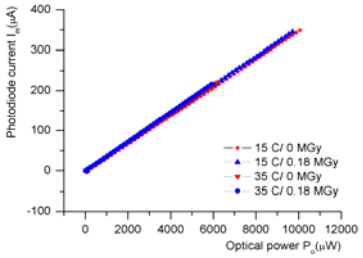

c

Figure 9. Irradiation effects on the laser diode emitting at 1300 nm: a -the optical power vs. the driving current characteristics; b – the direct voltage vs. the driving current characteristics; c – the photodiode current vs. the emitted optical power characteristics, for two gamma irradiation doses, at two case temperatures.

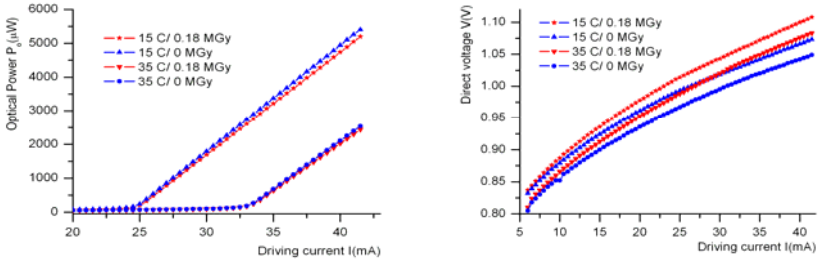

a *b*

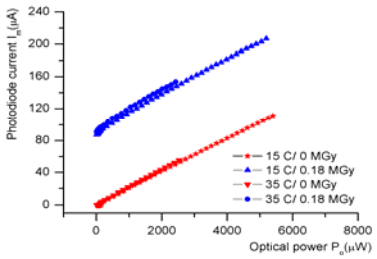

c

Figure 10. Irradiation effects on the laser diode emitting at 1550 nm: a -the optical power vs. the driving current characteristics; b – the direct voltage vs. the driving current characteristics; c – the photodiode current vs. the emitted optical power characteristics, for two gamma irradiation doses, at two case temperatures.

Under gamma irradiation the two laser diodes show a little change in their threshold currents and quite a good stability of the emitted optical power (better than 1 %). Problems are present after irradiation in relation to the increase of their direct voltage (i.e. 0.8 V at 40 mA driving current for the laser operating at 1300 nm) to degradation of their photodiodes.

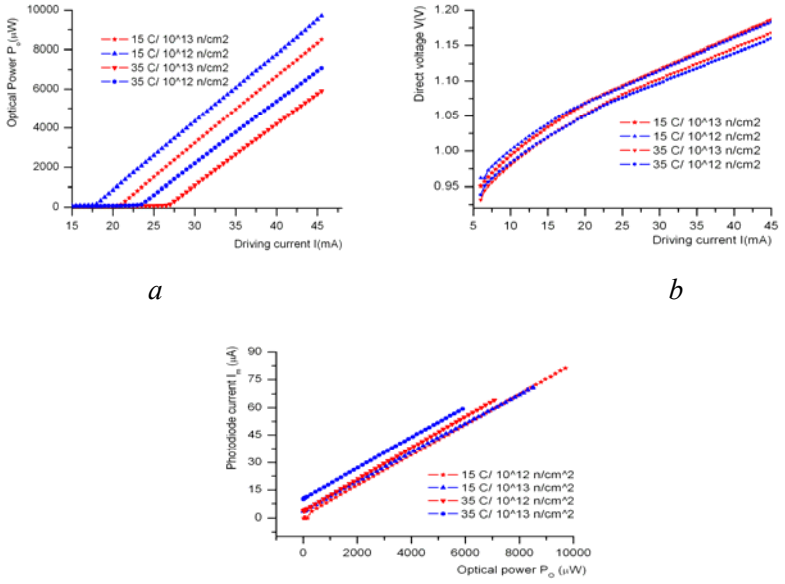

a *b*

c

Figure 11. Irradiation effects on the laser diode emitting at 1300 nm: a -the optical power vs. the driving current characteristics; b – the direct voltage vs. the driving current characteristics; c – the photodiode current vs. the emitted optical power characteristics, for two neutron fluences, at two case temperatures.

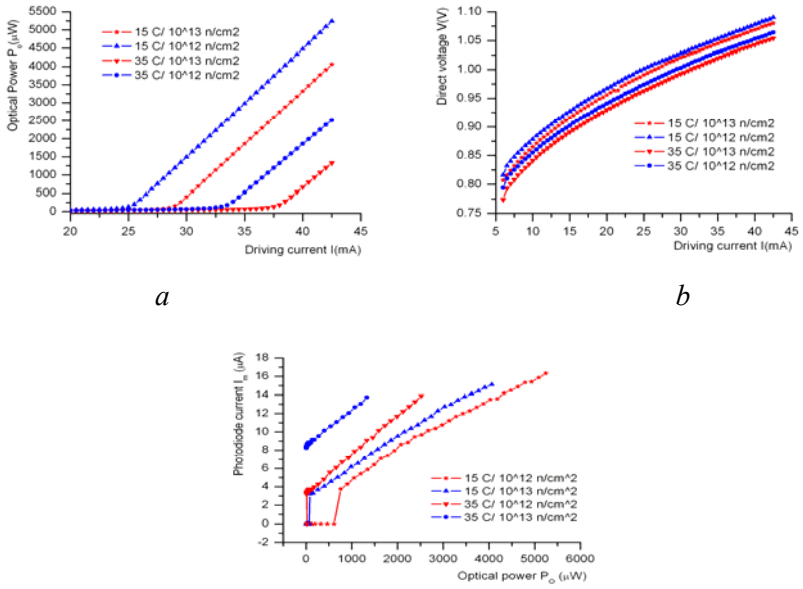

a *b*

c

Figure 12. Radiation effects on the laser diode emitting at 1550 nm: a -the optical power vs. the driving current characteristics; b – the direct voltage vs. the driving current characteristics; c – the photodiode current vs. the emitted optical power characteristics, for two neutron fluences, at two case temperatures.

In the case of neutron irradiation of the laser diodes operating at communication wavelengths significant changes can be observed in their threshold currents that increase (about 5 mA for the both lasers), and in the degradation of their photodiodes response. The most

affected was the laser operating at 1550 nm, case when the rise of the neutron fluence produces an increase of the dark current (from 3 μA at a fluence of 10^{12} n/cm^2 to more than 8 μA at a fluence of 10^{13} n/cm^2). Both lasers proved to have a stable optical power output (below 1 % as the fluence increases by 10 times).

2. Results concerning the irradiation of optical fibers

During the reporting period, several types of optical fibres were investigated as it concerns the change in their optical absorption in the UV – visible after the irradiation with gamma-ray and neutrons flux. All the optical fibres used in these experiments were of solarization resistant type, from the same manufacturer.

At this stage, silica optical fibres having core diameter of 200 μm, 600 μm and 1000 μm were tested. They are denoted in this report by OFS1 (200 μm), OFS2 (600 μm), OFS3 (600 μm) and OFS4 (1000 μm). The optical fibre designated as OFS3 has a better solarization resistance than the OFS2. The optical fibres OFS1 and OFS2 have the same composition, but different core diameters. All the optical fibres have an OH-doped core. The cladding of all optical fibres is of doped silica, while the jacket is of Polyimide. They can support up to 300 ^{O}C temperature stress. The evaluation was carried out on 25 cm long samples, in order to accommodate the volume available for irradiation. In this investigation all the measurements were done off-line; before and after each irradiation step the optical transmission of the samples was measured. In some cases, the optical fibre samples were heated between some irradiation steps and the optical transmission was measured. The cycles to which each optical fibre sample was subjected to are indicated for each Figure, for both gamma-ray irradiation and neutron irradiation. As an example, we indicate by **250C(4h) & 1kGy & 250C(4h) & 2 kGy** the following sequence: a heating to 250 ^{O}C for 4 hours, followed by a gamma irradiation at the dose of 1 kGy, followed by a heating for 4 hours at 250 ^{O}C, and a final irradiation at 2 kGy. The total irradiation dose received to a moment is the sum of all doses cumulated to that point.

The main results are given in Figures 13 – 17. All the representation for the optical absorption is expressed in logarithmic units.

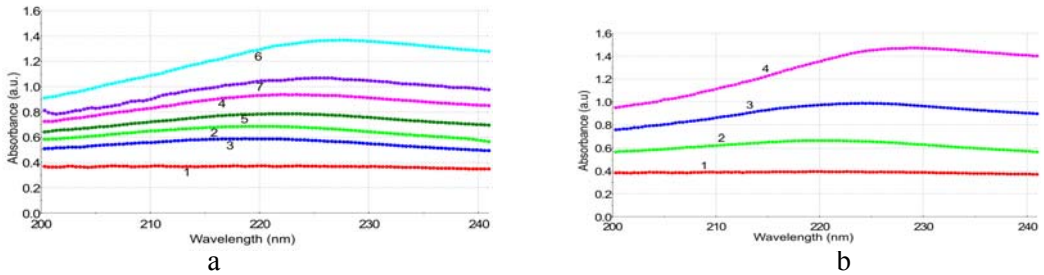

a b

*Figure 13. The irradiation induced absorption in the optical fibre OFS2, after it was subjected to the following processes (gamma-ray irradiation): 1 (red) – 250 ^{O}C; 2 (light green) – 250 ^{O}C & 1 kGy; 3 (blue) – 250 ^{O}C & 1 kGy & 250 ^{O}C; 4 (magenta) – 250 ^{O}C & 1 kGy & 250 ^{O}C & 2 kGy; 5 (dark green) – 250 ^{O}C & 1 kGy & 250 ^{O}C & 2 kGy & 250 ^{O}C; 6 (cyan) – 250 ^{O}C & 1 kGy & 250 ^{O}C & 2 kGy & 250 ^{O}C & 10 kGy; 7 (violet) – 250 ^{O}C& 1 kGy & 250 ^{O}C & 2 kGy & 250 ^{O}C & 10 kGy & 250 ^{O}C **(a)**; the radiation induced absorption in the optical fibre OFS2, after it was subjected to the following processes (gamma-ray irradiation): 1 (red) – non irradiated; 2 (light green) – 1 kGy; 3 (blue) – 2 kGy; magenta – 10 kGy **(b)**.*

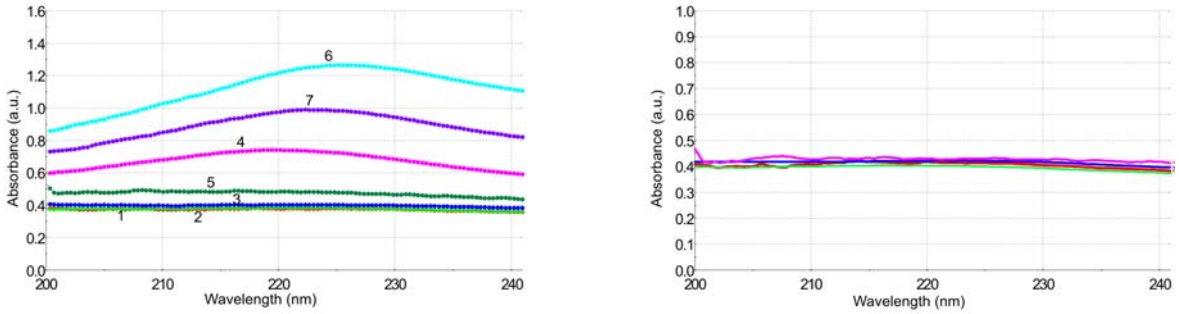

a b

*Figure 14. The irradiation induced absorption in the optical firer OFS3, after it was subjected to the following processes (gamma-ray irradiation): 1 (red) – 250 ^{O}C; 2 (light green) – 250 ^{O}C & 1kGy; 3 (blue) – 250 ^{O}C & 1 kGy & 250 ^{O}C; 4 (magenta) – 250 ^{O}C & 1 kGy & 250 ^{O}C& 2 kGy; 5 (dark green) – 50 ^{O}C & 1 kGy & 250 ^{O}C & 2 kGy & 250 ^{O}C; 6 (cyan) – 250 ^{O}C & 1 kGy & 250 ^{O}C& 2 kGy & 250 ^{O}C& 10 kGy; 7 (violet) – 250 ^{O}C & 1 kGy & 250 ^{O}C & 2 kGy & 250 ^{O}C & 10 kGy & 250 ^{O}C (**a**); the radiation induced absorption in the optical fibre OFS3, after it was subjected to the following processes (gamma-ray irradiation): 1 (red) – non irradiated; light green – 1 kGy; 2 (blue) – 2 kGy; 3 (magenta) – 10 kGy (**b**).*

Figure 13 indicates a recovery phenomenon observed after the optical fibre was subjected to several heating steps. The recovery produces also a decrease of the peak absorption wavelength. In the mean time, the maximum value of the absorption peak is diminished also by temperature cycling. In Figure 14 can be observed that the optical fibre denoted by OFS3 is the most radiation resistant one, as its absorption does not change even at total irradiation doses of 10 kGy. Its radiation hardening is reduced if the optical fibre is heated previous to the first irradiation step. In this situation its behaviour is similar to that of the optical fibre OFS2.

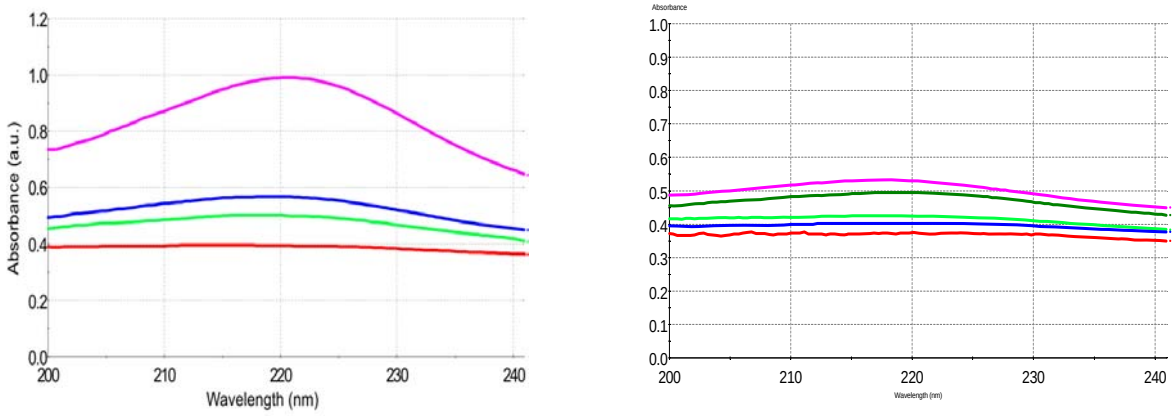

a b

*Figure 15. The irradiation induced absorption in the optical fibre OFS4, after it was subjected to the following processes (gamma-ray irradiation): 1 (red) – non irradiated; 2 (light green) – 1 kGy; 3 (blue) – 2 kGy; 4 (magenta) – 10 kGy (**a**); the radiation induced absorption in the optical fibre OFS2, after it was subjected to the following processes (neutron irradiation): 1 (red) – 250 ^{O}C (4h); 2 (light green) – 250 ^{O}C (4h) & 6x10^{11} n/cm^2; 3 (blue) – 250 ^{O}C (4h) & 6x10^{11} n/cm^2 & 250 ^{O}C (4h); 4 (magenta) – 250 ^{O}C (4h) & 6x10^{11} n/cm^2 & 250 ^{O}C (4h) & 6x10^{12} n/cm^2; 5 (dark green) – 250 ^{O}C (4h) & 6x10^{11} n/cm^2 & 250 ^{O}C (4h) & 6x10^{12} n/cm^2 & 250 ^{O}C (4h) (**b**).*

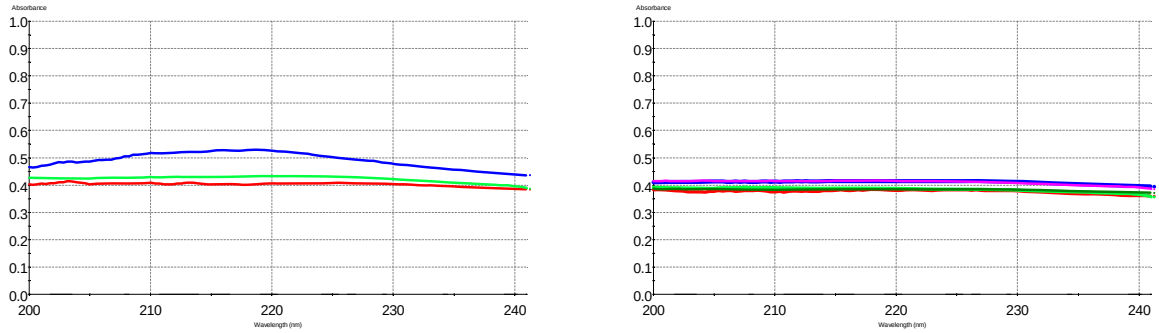

a b

*Figure 16. The irradiation induced absorption in the optical fibre OFS2, after it was subjected to the following processes (neutron irradiation): 1 (red) – non irradiated; 2 (light green) – $6x10^{11}$ n/cm^2; 3 (blue) – $6x10^{12}$ n/cm^2 (**a**); the radiation induced absorption in the optical fibre OFS3, after it was subjected to the following processes (neutron irradiation): 1 (red) – 250^{O}C (4h); 2 (light green) – 250 ^{O}C (4h) & $6x10^{11}$ n/cm^2; 3 (blue) – 250 ^{O}C (4h) & $6x10^{11}$ n/cm^2 & 250 ^{O}C (4h); 4 (magenta) – 250 ^{O}C (4h) & $6x10^{11}$ n/cm^2 & 250 ^{O}C (4h) & $6x10^{12}$ n/cm^2; 5 (dark green) – 250 ^{O}C (4h) & $6x10^{11}$ n/cm^2 & 250 ^{O}C (4h) & $6x10^{12}$ n/cm^2 & 250 ^{O}C (4h) (**b**).*

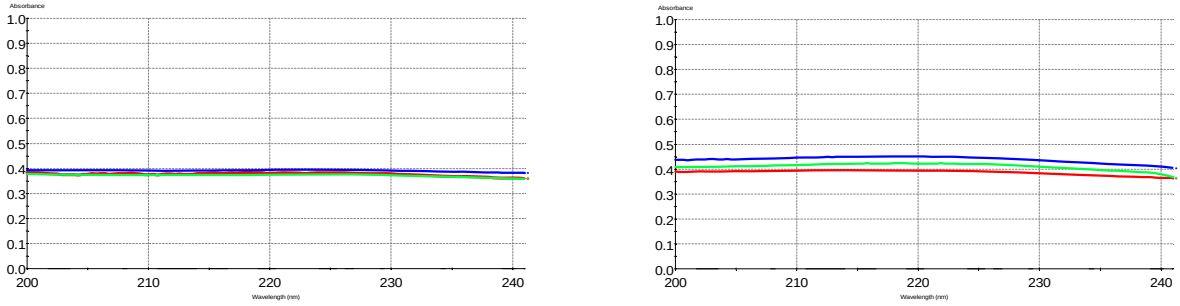

a b

*Figure 17. The radiation induced absorption in the optical fibre OFS3, after it was subjected to the following processes (neutron irradiation): 1 (red) – non irradiated; 2 (light green) - $6x10^{11}$ n/cm^2; 3 (blue) – $6x10^{12}$ n/cm^2(**a**); The radiation induced absorption in the optical fibre OFS4, after it was subjected to the following processes (neutron irradiation): 1 (red) – non irradiated; 2 (light green) – $6x10^{11}$ n/cm^2; 3 (blue) – $6x10^{12}$ n/cm^2 (**b**).*

Figures 15 *b* and 16 *a* reveal the influence of the heating process between neutron irradiation steps. As in the case of gamma irradiation a partial recovery phenomenon can be observed. As in the case of gamma irradiation the optical fibre OFS2 proves to be more radiation resistant than other optical fibres (Figure 16 *b*). Comparing the optical fibres OFS3 and OFS4 (Figure 17) after neutron irradiation a high radiation resistance can be noticed in the case of OFS3.

In order to assess the quality of the solarization resistant optical fibres as compared to non-solarization resistant ones a study is illustrated in Figure 18. In Figure 18 *a* all the optical fibres have a 600 μm core diameter, while the optical fibres in Figure 18 *b* have a 1000 μm core diameter.

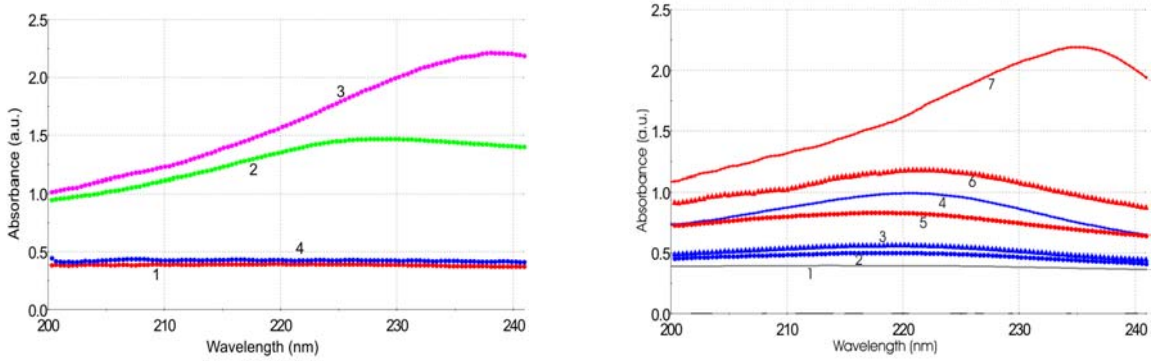

a b

*Figure 18. The optical absorption for: 1 (red) – non-irradiated, solarization resistant OFS3 optical fibre; 2 (green) – irradiated solarization resistant OFS2 optical fibre; 3 (magenta) – irradiated non-solarization resistant optical fibre; 4 (blue) – irradiated solarization resistant OFS3 optical fibre. Total irradiation dose: 13 kGy (**a**); the optical absorption for: 1(gray) – non-irradiated, solarization resistant OFS4 optical fibre; 2 (blue dot) – solarization resistant OFS4 optical fibre irradiated at the total dose of 1 kGy; 3 (blue triangle) – solarization resistant OFS4 optical fibre irradiated at the total dose of 3 kGy; 4 (blue star) – solarization resistant OFS4 optical fibre irradiated at the total dose of 13 kGy; 5 (red dot) – non-solarization resistant optical fibre irradiated at the total dose of 1 kGy; 6 (red triangle) – non-solarization resistant optical fibre irradiated at the total dose of 3 kGy; 7 (red star) – non-solarization resistant optical fibre irradiated at the total dose of 13 kGy (**b**).*

The solarization resistant optical fibre proved to be more radiation resistant than the optical fibres with an enhanced UV response. In the mean time, a shift of the peak absorption wavelength towards high values can be noticed with the increase of the total dose, as new colour centres are generated.

References:

[1]. **Sporea D.**, "*Effects of Gamma-Ray Irradiation on Quantum-Well Semiconductor Lasers*", Nuclear and Space Radiation Effects Conference, Atlanta, July 21 - 23, 2004, to be published at IEEE Proceedings "Radiation Database".

[2]. **Dan G. Sporea**, **Constantin Oproiu**, **Radu A. Sporea**, "*Degradation of heterojunction laser diodes under electron beam irradiation*", Photonics North Conference 2004, Ottawa, September 21 – 24, 2004, to be published as a SPIE Proceedings.

[3]. **Sporea D.**, "*Update on the evaluation of radiation effects on optical fibres and semiconductor lasers*", 7th Meeting of the ITPA TG on Diagnostics, Hefei, 11 - 14 October, 2004.

[4]. **Sporea D.**, **Adelina Sporea**, **and Constantinescu B.**, "*Optical fibres for plasma diagnostics under gamma-ray and UV irradiation*", Symposium on Fusion Technology, September 18 – 21, 2004, Venice, submitted for publication to Fusion Engineering and Design.

[5]. **Sporea D.**, "*Prospects for optical fibres below 400 nm*", IEA Satellite Meeting, September 24, 2004, Venice.